

Surface Plasmon Interference Fringes in Back-Reflection

A. Drezet, A. L. Stepanov, A. Hohenau, B. Steinberger, N. Galler,
H. Ditlbacher, A. Leitner, F. R. Aussenegg, and J. R. Krenn
Institut of physics, Karl-Franzens University Graz, Universitätsplatz 5 A-8010 Graz, Austria

M. U. Gonzalez, and J.-C. Weeber
*Laboratoire de Physique de l'université de Bourgogne, UMR CNRS 5027,
9 Avenue A. Savary, BP 47870, F-21078 Dijon, France*
(Dated: November 14, 2018)

We report the experimental observation of surface plasmon polariton (SPP) interference fringes with near-unity visibility and half-wavelength periodicity obtained in back reflection on a Bragg mirror. The presented method based on leakage radiation microscopy (LRM) represents an alternative solution to optical near-field analysis and opens new ways for the quantitative analysis of SPP fringes. With LRM we investigate various SPP interference patterns and analyze the high reflectivity of Bragg mirror in comparison with theoretical models.

PACS numbers: 78.67.-n

The development of optics at the micron and sub-micron scales requires the control over coherence of wave propagation in a confined environment as well as the knowledge of the optical properties of the structures used for this purpose. In this context the recent progresses in surface plasmon polariton (SPPs) [1] optics allowed the realization of optical elements as Bragg mirrors and beam splitters. These elements have been combined in various 2D SPP devices like a Mach-Zehnder interferometer [2], or an elliptical resonator [3]. In order to achieve SPP mirrors with very high reflectivity one has to study quantitatively the interaction of SPP waves and Bragg reflectors. In this context the quantitative near-field measurement of the reflectivity of Bragg mirrors integrated into SPP waveguides [4, 5] was reported. Here we propose an alternative method of analysis based on far-field leakage radiation microscopy (LRM) that we developed recently into a systematic routine [6]. For this purpose we consider the back-reflection of propagating SPP waves impinging normally onto a Bragg mirror. In order to show the accuracy of the method we report experimental evidence for interference between incident and back-reflected SPP wave with a periodicity of $\lambda_{SPP}/2$ (λ_{SPP} being the SPP wavelength) and with a quasi-unity fringe visibility $V \simeq 1$. We show that the results are consistent with the theoretical expectations and with an ideal SPP reflectivity of 100%. This in turn proves that back-reflection can be a useful tool for the local tailoring of the SPP intensity pattern by interference of incident and reflected SPP beams. The Bragg mirror structures are constituted by a set of 20 parallel gold ridges (70 nm height, 150 nm width) fabricated by electron beam lithography (EBL) on glass substrate [4]. The distance between the ridges is $d = \lambda_{SPP}/2 = 390$ nm (see Fig. 1a). At normal incidence this corresponds to Bragg reflectance maxima for a laser wavelength $\lambda_0 \simeq \lambda_{SPP}$ of 780 nm (Ti:sapphire). SPP waves are locally launched from an additional ridge (150

nm width) located in front of the Bragg reflector at a distance of $\simeq 30$ μm (see Fig. 1a). The laser beam is focused onto this ridge using a microscope objective (50 \times , numerical aperture 0.7) and the laser spot diameter is around 2 μm which corresponds to a full divergence angle θ of the SPP beam on the gold film of about 32 $^\circ$. The SPP wave propagating to the left impinges normally on the Bragg mirror and is reflected back to the right giving rise to an interference pattern. Fig. 1b shows a LRM image [3, 6] of the SPP propagation obtained using an oil immersion objective (63 \times , numerical aperture=1.25). The absence of SPP transmittance behind the Bragg mirror leads to the conclusion that the incident SPP wave is mostly back-reflected. The diffraction behavior visible to the right of the launching ridge can be straightforwardly understood as a result of the interference between the SPP wave originating from the ridge and a virtual image-source located in the half-space to the left of the Bragg mirror. This is confirmed theoretically by simulating the SPP propagation with a simple scalar wave model [3] (see Fig. 2). The SPP field launched at the ridge is modelled by a continuous distribution of 2D dipoles whose orientation is in the sample plane and normal to the ridge direction. To simplify the calculation we considered a SPP mirror consisting of a single ridge located at the position of the Bragg reflector. The interaction of the incident SPP beam with this ideal mirror generates secondary SPP waves interfering with the incident beam to generate the observed lateral interference patterns to the right of the ridge. It is observed that despite the high value of the divergence angle θ the observed reflectivity is very high. This shows qualitatively that the reflectivity of this Bragg mirror is not very sensible to the incidence angle α in a domain $\Delta\alpha \simeq \pm 10^\circ$. This effect has already been observed in the near-field experiments mentioned [4] and can be explained if we suppose that a periodical grating opens a gap in the angular dispersion curve of SPPs [7]. In or-

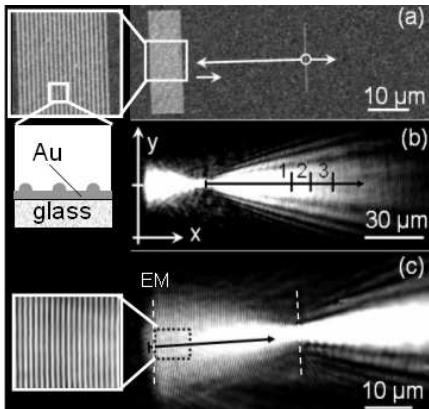


FIG. 1: (a) Scanning electron microscope (SEM) image of Bragg mirror and launching ridge. The insets shows a zoom on the Bragg mirror and a sketch of the mirror structure. SPPs are launched from the ridge region contained in the white circle and propagate normally to the ridge as represented by the arrows. The left SPP beam is back-reflected by the mirror. (b) LRM image of SPP interference pattern. The black arrow and the marks 1,2,3 refer to cross-cuts in Fig. 3. (c) LRM image at higher magnification allowing the observation of interference fringes between mirror and ridge. The black arrow refers to the cross-cut in Fig. 4. The inset shows a zoom of the fringes. The white dotted lines show the position of the ridge and of the effective Bragg mirror (EM) (see Fig. 4).

der to analyze the SPP propagation we extracted different cross-cuts of the LRM images. The three transversal cross-cuts represented in Figs. 3a, b and c correspond to the directions and positions indicated in Fig. 1b. Fig. 3d shows a longitudinal cross-cut along the SPP propagation direction in Fig. 1b. Altogether these cross-cuts agree

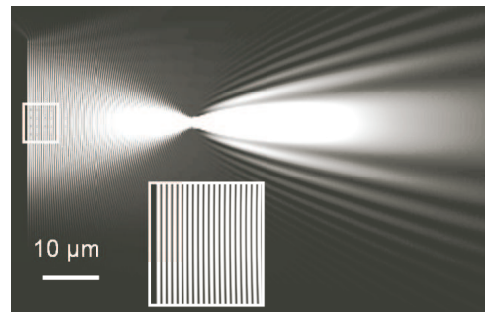


FIG. 2: Theoretical simulation of the SPP interference pattern in Fig. 1. The model relies on scalar waves as discussed in the text. The inset shows the SPP fringes at higher magnification.

very well with the simulation if we adjust adequately the SPP propagation length L_{SPP} and the effective mirror reflectivity R which are the two free parameters of the model. Both transversal and longitudinal cross-cuts are necessary for fixing R and L_{SPP} . We find the best fit with a total reflectivity $R \simeq 95 \pm 5\%$ and $L_{\text{SPP}} \simeq 26\mu\text{m}$ which agrees with the value expected for a gold film [1]. To understand the physical meaning of the R value we now focus our attention on the remarkable interference features present in the region between the Bragg reflector and the launching ridge. Indeed, in this region, as shown in the simulation (see inset on Fig. 2), one expects theoretically interferences fringes with very high contrast $V = (I_{\text{max}} - I_{\text{min}})/(I_{\text{max}} + I_{\text{min}})$ close to one. We note that this effect is not visible in Fig. 1b, since this figure is resolution limited due to the finite size of the pixels on the charged-coupled-device camera used to acquire the image. By increasing the magnification of the LRM [8] we however overcome this limit and we observe fringe interference with a periodicity of 390 nm corresponding to $\lambda_{\text{SPP}}/2$ (see Fig. 1c). This observation can seem rather surprising if we think of Rayleigh diffraction limiting the spatial resolution to $\sim \lambda_0/(2NA) \simeq \lambda_{\text{SPP}}/2.5$ with $NA = 1.25$, the oil immersion objective numerical aperture. One should intuitively thus expect that the fringes will be blurred in the image plane, as indeed incoherent optics predicts a reduced visibility below 10% [9]. However, the SPP standing wave pattern is a coherent phenomenon and it can be proven using Fourier optics and Abbe's theory [10] that the diffraction limit does not affect the visibility V [11]. In the present case the immersion objective has a high numerical aperture and we estimate that the unity fringe visibility existing in the sample plane conserves its value in the image plane where we expect thus $V_{\text{exp}} \simeq 1$.

In order to analyze the fringes we plot a cross-cut in the direction indicated by the black arrow in Fig. 1c. This cross cut is depicted in the inset of Fig. 4. The red curve shows the averaged intensity as simulated by the theoretical model which reproduces the general trend of the

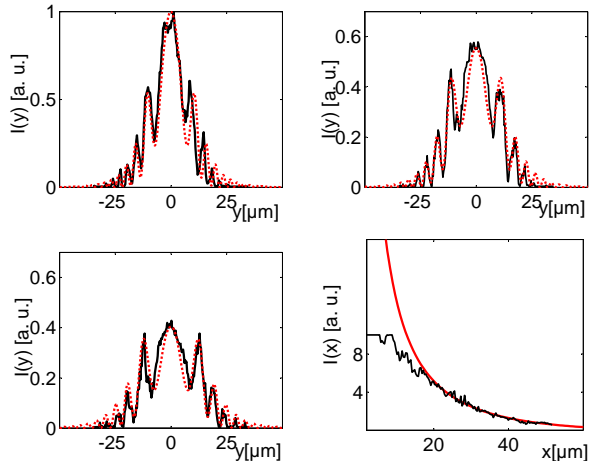


FIG. 3: (color online) (a-c) Transversal cross-cuts of the SPP intensity corresponding to the marks 1,2,and 3 in Fig. 1b respectively. The experimental data (black curves) and the model (red dashed curves) are compared. The origin of the y axis is given by a white mark on the y axis of Fig. 1b (d) Longitudinal cross-cuts along the direction indicated by an arrow in Fig. 1b. The origin of the arrow corresponds to the origin of the cross-cut. Experimental data (black curve) and theory (red curve) are compared.

intensity profile quite well. The agreement is however not limited to the averaged intensity as visible from the main curve of Fig. 4 which zooms a detail of the inset close to the Bragg mirror. The oscillation fringes observed experimentally coincide with the theoretical predictions and in particular reproduce the very high contrast expected in this region. A simple way to calculate the reflectivity R is to consider the ideal standing wave pattern obtained using two counter propagative plane waves leading to the intensity $I(x) \simeq 1 + V_{\text{ideal}} \cos(4\pi x/\lambda_{\text{SPP}} + \text{const.})$ with $V_{\text{ideal}} = 2\sqrt{R}/(1+R)$. Since this plane wave hypothesis can be considered as valid in the vicinity of the Bragg mirror boundary we deduce that R should equal $95 \pm 5\%$. The uncertainty is partly a result of the microscope diffraction limit discussed before. It can be added that the consistency of the argumentation is ex-

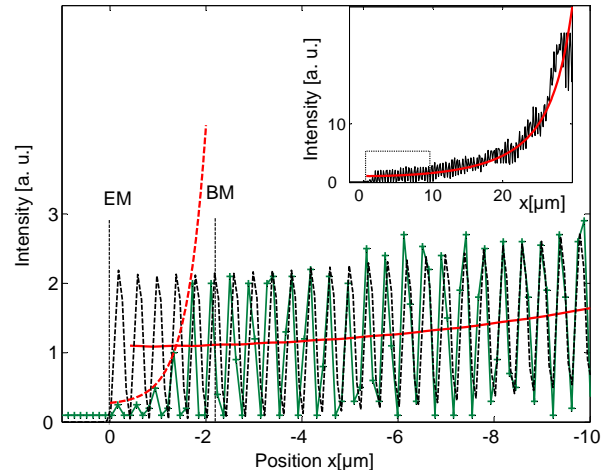


FIG. 4: (color online) Cross-cut of the interference fringes (green curve) along the direction represented by the black arrow of Fig. 1c (the origin of the cross-cut axis corresponds to the origin of the arrow). The red curve shows the averaged intensity as predicted by the model and the black dashed curve shows the predicted interference. The red dashed curve is the exponential fit for the effective plasmon damping starting at the beginning of Bragg's mirror (BM) and finishing at the position of the effective mirror (EM). The inset shows a larger view of the interference (black curve) as well as the predicted averaged intensity (red curve).

perimentally confirmed by the fact that an incoherent illumination of the sample with an external light source (not shown) does not allow us to resolve the separation between the ridges constituting the Bragg mirror. Since the periodicity of the fringes equals the one of the Bragg mirror it indeed proves that an incoherent effect can not be invoked as a justification for the quasi-unity fringes visibility observed with SPPs. From these results and from the experimental fact that no SPP is transmitted through the Bragg mirror (see Figs. 1 and 4) one can thus conclude that 1) the transmission T is below the noise level, i. e., below 0.5% and 2) that a few percent of the the incident SPP beam (i. e., $S=5-10\%$) are scattered to light into the glass substrate, this to accord to

energy conservation. It can be finally remarked that the mirror model used in this work did not consider, to simplify the problem, the precise structure of the Bragg mirror. This explains why in order to reproduce accurately the experimental observation we must position precisely the effective mirror (EM in Fig. 4) $2 \mu\text{m}$ to the left of the physical boundary corresponding to the first ridge of the Bragg mirror (BM in Fig. 4). The experimentally observed effective damping inside of Bragg's mirror can be physically understood if we consider that a SPP wave needs to propagate inside of the periodical structure before being reflected back. This damping can be well approximated by an exponential decay law whose propagation length δ is around 500 nm.

In summary, we have presented an accurate method to measure reflectivity for SPP Bragg mirrors in normal incidence. The method based on LRM imaging allows the observation of standing wave fringes with a periodicity as small as $\lambda_{\text{SPP}}/2$ and with a high contrast close to unity. The method due its sensibility constitutes a good complement to near-field measurements made on the same kind of structures [5]. In all cases the observations are in good quantitative agreement with the theoretical expectations and show that the essential behaviors are well understood.

For financial support the European Union, under projects FP6 NMP4-CT-2003-505699 and the Lisa Meitner programm of the Austrian Science Foundation (M868-N08) are acknowledged.

-
- [1] H. Raether, *Surface Plasmons*(Springer, Berlin, 1988).
 [2] H. Ditlbacher, J. R. Krenn, G. Schider, A. Leitner, and F. R. Aussenegg, Appl. Phys. Lett. **81**, 1762 (2002).
 [3] A. Drezet, A. L. Stepanov, H. Ditlbacher, A. Hohenau, B. Steinberger, F. R. Aussenegg, A. Leitner, and

- J. R. Krenn, Appl. Phys. Lett. **86**, 074104 (2005).
 [4] J.-C. Weeber, M. U. González, A.-L. Baudrion, and A. Dereux, Appl. Phys. Lett. **87**, Appl. Phys. Lett. **87**, 1 (2005).
 [5] J.-C. Weeber, Y. Lacroute, A. Dereux, E. Devaux, T. Ebbesen, C. Girard, M. U. González, and A.-L. Baudrion, Phys. Rev. B **70**, 235406 (2004).
 [6] A. Stepanov, J. R. Krenn, H. Ditlbacher, A. Hohenau, A. Drezet, B. Steinberger, A. Leitner, and F. Aussenegg, Opt. Lett. **30**, 1524 (2005).
 [7] W. L. Barnes, S. C. Kitson, T. W. Presit, and J. Sambles, J. Opt. Soc. Am. A **14**, 1654 (1997).
 [8] By increasing by a factor 5 the focal length of the imaging lens located in front of the CCD camera (see [6]) we multiply the microscope magnification by the same factor.
 [9] From incoherent optics the original intensity pattern $I_0(\mathbf{x})$ (where $\mathbf{x} = [x, y]$ is the 2D position vector) is convoluted with the impulse response function of the objective $F^2(\mathbf{x}) = [2J_1(k|\mathbf{x}|NA)/(k|\mathbf{x}|NA)]^2$. For the intensity pattern in the image plane one has $I_i(\mathbf{x}) \propto \int F^2(\mathbf{u}) \cdot I_0(\mathbf{u} - \mathbf{x}/M)d^2\mathbf{u}$ with M the absolute value of the transverse microscope magnification. If $I_0(\mathbf{x}) = 1 + \cos(2\mathbf{k} \cdot \mathbf{x})$ one obtains $I_i(\mathbf{x}) \propto 1 + V \cos(2\mathbf{k} \cdot \mathbf{x}/M)$ with $V \simeq e^{2 \cdot (1.4/NA)^2} \simeq 9\%$ (we used the numerical approximation $[2J_1(u)/u]^2 \approx e^{-\frac{1}{2}(u/1.4)^2}$).
 [10] M. Born and E. Wolf, *Principles of optics, seventh (expanded) edition* (Cambridge University Press, Cambridge, 1999).
 [11] For the electric field of a coherent SPP wave which in the object plane has the form $f_0(\mathbf{x}) = e^{i\mathbf{k} \cdot \mathbf{x}} + \mathcal{R} \cdot e^{-i\mathbf{k} \cdot \mathbf{x}}$ ($R = |\mathcal{R}|^2$ is the Bragg mirror reflectivity) one obtains in the image plane $f_i(\mathbf{x}) \propto \int F(\mathbf{u}) \cdot f_0(\mathbf{u} - \mathbf{x}/M)d^2\mathbf{u}$, e. g. , the convolution of f_0 with the impulse response of the objective for the field $F(\mathbf{x}) = 2J_1(k|\mathbf{x}|NA)/(k|\mathbf{x}|NA)$ (compare [9]). Since $F(\mathbf{x}) = F(-\mathbf{x})$ one deduces $f_i(\mathbf{x}) \propto e^{-i\mathbf{k} \cdot \mathbf{x}/M} + \mathcal{R} \cdot e^{i\mathbf{k} \cdot \mathbf{x}/M}$. It implies $I_i(\mathbf{x}) = |f_i(\mathbf{x})|^2 \propto 1 + V \cos(2\mathbf{k} \cdot \mathbf{x}/M + \text{const.})$ with the same visibility $V = 2\sqrt{R}/(1 + R)$ than the SPP wave intensity $I_0(\mathbf{x}) = |f_0(\mathbf{x})|^2 \propto 1 + V \cos(2\mathbf{k} \cdot \mathbf{x} - \text{const.})$.